Title

Cationic liposome—nucleic acid complexes: liquid crystal phases with applications in gene therapy

Journal

Liquid Crystals, 38(11-12)

ISSN

0267-8292

Authors

Safinya, CR

Ewert, KK

Leal, C

Publication Date

2011-11-01

DOI

10.1080/02678292.2011.624364

Published in final edited form as:
Liq Cryst. 2011 ; 38(11-12): 1715–1723. doi:10.1080/02678292.2011.624364.

Cationic liposome-nucleic acid complexes: liquid crystal phases with applications in gene therapy

C. R. Safinya[*], **K. K. Ewert**, and **Cecília Leal**
Materials Department, Physics Department, and Molecular, Cellular, & Developmental Biology Department, University of California, Santa Barbara, CA 93106, USA

Abstract

Cationic liposome (CL) carriers of nucleic acids are primarily studied because of their applications in gene delivery and gene silencing with CL-DNA and CL-siRNA (short-interfering RNA) complexes, respectively, and their implications to ongoing clinical gene therapy trials worldwide. A series of synchrotron-based small-angle-x-ray scattering studies, dating back to 1997, has revealed that CL-nucleic acid complexes spontaneously assemble into distinct novel liquid crystalline phases of matter. Significantly, transfection efficiency (TE; a measure of expression of an exogenous gene that is transferred into the cell by the lipid carrier) has been found to be dependent on the liquid crystalline structure of complexes, with lamellar complexes showing strong dependence on membrane charge density (σ_M) and non-lamellar complexes exhibiting TE behavior independent ofσ_M. The review describes our current understanding of the structures of different liquid crystalline CL-nucleic acid complexes including the recently described gyroid cubic phase of CL-siRNA complexes used in gene silencing. It further makes apparent that the long-term goal of developing optimized liquid crystalline CL-nucleic acid complexes for successful medical applications requires a comprehensive understanding of the nature of the interactions of distinctly structured complexes with cell membranes and events leading to release of active nucleic acids within the cell cytoplasm.

Keywords

cationic liposomes; gene delivery; nucleic acids; short-interfering RNA; lamellar complexes; hexagonal complexes; cubic complexes; small-angle-x-ray-scattering

1. Introduction

The interest in cationic liposomes (CLs, closed bilayer membrane shells of lipid molecules; figure 1) as gene carriers (or vectors) in gene therapy applications is currently unprecedented [1–10]. Indeed the entire field of gene therapy based on synthetic nonviral delivery systems has undergone a renaissance since the initial paper by Felgner et al. [11] where it was found that cationic liposomes, when mixed with DNA to form CL-DNA complexes with an overall positive charge, result in transfection efficiencies (TE; a measure of expression of an exogenous gene that is transferred into the cell by the lipid carrier) significantly higher than other chemical-delivery systems (e.g. anionic liposomes with encapsulated DNA, calcium-phosphate precipitation, and polycationic reagents such as DEAE-dextran or polylysine) [11]. They hypothesized that the improved TE was because DNA chains attached to cationic liposomes (figure 1, top) would be effectively anchored to the cell surface through the electrostatic adsorption of CLs onto the anionic sulfated-proteoglycan coating of

[*]Corresponding author. safinya@mrl.ucsb.edu.

mammalian cells. This landmark publication was soon followed by other groups demonstrating CL-DNA based gene expression in human clinical trials [12] and currently out of a total of about 1700 ongoing clinical trials worldwide, targeting both single gene diseases (e.g. cystic fibrosis) and complex multi-gene diseases such as cancer, 6.4% (109 trials) use CL-DNA based "lipofection" methods (figure 1) [13,14].

In contrast to synthetic vectors, engineered viral vectors are typically far more efficient in gene therapy applications; however, they are also far less safe. Use of engineered adenoviral and retroviral vectors have, respectively, resulted in severe immune reactions with two patient deaths and insertional mutagenesis leading to cancer in two patients in a small trial with patients treated for X-linked SCID (severe combined immunodeficiency) [15–17]. The relative safety of lipofection is because no viral genes are present to cause disease, and furthermore, the lack of proteins makes the synthetic vector relatively non-immunogenic.

Another exciting advantage of synthetic vectors compared to engineered viral vectors for gene delivery is the potential of transferring and expressing large pieces of DNA into cells. Experiments have shown that partial sections of human artificial chromosomes (HACs) of order 1 Mbp may be transferred into cells with CL-vectors, although extremely inefficiently [18, 19]. In contrast engineered viruses have a maximum carrying load of order 20 kbp to 30 kbp due to the finite size of their capsid. The future development of readily useable HAC vectors will signal a turning point for the field of synthetic gene therapy. Because of their very large size capacity HACs would have the ability of delivering (e.g. via CL-vectors) not only entire human genes but also their regulatory sequences for the spatial and temporal regulation of expression (requiring DNA sections often exceeding 100 kbp per gene).

While transfection efficiency have been found to be enhanced using CL-DNA complexes compared to other more traditional synthetic delivery systems, the mechanism of transfection via cationic liposomes remains poorly understood [1–10]. Transfection efficiencies with lipid carriers will only be optimized after the development of a comprehensive understanding of the interactions of CL-DNA complexes with cell membranes and other components such as the cytoskeleton network, which lead to cytosol delivery of complexes followed by DNA release and gene expression.

2. The lamellar L_{α}^{C} and inverse hexagonal H_{II}^{C} phases of cationic liposome-DNA complexes

The first liquid crystalline phase of CL-DNA complexes was discovered in an x-ray study where cationic liposomes (≈ 50 nm diameter), consisting of mixtures of neutral lipid DOPC (di-oleoyl phosphatidyl cholin) and univalent cationic lipid DOTAP (di-oleoyl trimethylammonium propane) (figure 2), were complexed with linear lambda-phage DNA (48 Kb) [20]. High resolution synchrotron small-angle-x-ray-scattering (SAXS) unambiguously demonstrated that the structure is different from the hypothesized "bead-on-string" structure, proposed by Felgner et al. for CL-DNA complexes in their seminal paper [11], picturing the DNA strand decorated with distinctly attached cationic liposomes (figure 1).

The complexation of cationic liposomes with oppositely charged DNA led spontaneously to the formation of dense globules with average diameter between 100 nm and 200 nm measured by dynamic light scattering. Polarized microscopy showed that the globules were birefringent indicative of their liquid crystalline nature [20]. SAXS data of dilute (volume fraction of water ≈ 99%) DOPC/DOTAP (1:1 wt.:wt.) -λ-DNA mixtures as a function of L/D (L = DOPC + DOTAP) (figure 3, left) were consistent with a complete topological rearrangement of liposomes and DNA into a multilayer structure with DNA intercalated

between the bilayers (figure 3, right, labeled L_α^C) [20]. Two sharp peaks at q = 0.098 $Å^{-1}$ and 0.196 $Å^{-1}$ correspond to the (001) and (002) peaks of a layered structure with an interlayer spacing d (= $\delta_m + \delta_w$) = 64 Å. Here, δ_m and δ_w, are the membrane thickness and water gap respectively (figure 3, right). The membrane thickness was independently measured by a well-known SAXS technique where the unit cell spacing in multilamellar membranes is measured as a function of increasing volume fraction of water in the one-phase lamellar L_α phase [21–24]. For the case of DOTAP:DOPC (1:1 wt.:wt.) δ_m was found to be 39 Å [20]. Thus, the water layer thickness$\delta_w = d - \delta_m$ = 25 Å, was found to accommodate one monolayer of B-DNA (diameter ≈ 20 Å) including a hydration shell.

The middle broad peak q_{DNA} (figure 3, left) arises from DNA-DNA correlations and gives the interaxial spacing $d_{DNA} = 2\pi/q_{DNA}$. For isoelectric complexes prepared at L/D = 7, d_{DNA} = 47.5 Å [20]. Quantitative line-shape analysis of the DNA correlation peak has shown that the DNA chains form a finite-size 1D array of chains (i.e. a 2D smectic phase) with the DNA electrostatically adsorbed to the cationic membrane [25, 26]. The spacing d_{DNA} was found to increase from ≈ 25 Å (i.e. close packing of chains at DOTAP/DNA = 2.2 with no added neutral lipid DOPC) at high membrane charge density, to an expanded 2D smectic phase with d_{DNA} ≈ 55 Å at low membrane charge density (L/D = 9, DOTAP/DNA = 2.2) [20, 27, 28].

Thus, we see that the lamellar L_α^C phase of CL-DNA complexes is a novel hybrid liquid crystalline phase: the lipids form a three-dimensional smectic phase [21–24] while the DNA rods between the lipid bilayers form a two-dimensional smectic phase [29, 30]. The multilamellar L_α^C structure with intercalated DNA is also observed in CL-DNA complexes containing circular plasmid DNA (i.e. gene containing DNA) both in water, and also in Dulbecco's Modified Eagle Medium used in cell transfection experiments [31]. It is interesting to point out that theory of the lamellar phase of CL-DNA complexes also predicts the existence of a novel “sliding columnar” phase, an entirely new phase of matter, where the DNA rods have long-range orientation order from layer to layer but are not positionally correlated between layers [32–34].

The driving force for the spontaneous self-assembly of CLs and DNA into the lamellar L_α^C liquid crystalline phase is the release of positive counterions that are bound to free DNA (referred to as Manning condensation [35]) and negative counterions near the cationic liposome surface within the Guoy-Chapman layer [36]. During condensation, the cationic membrane neutralizes the phosphate groups on the DNA in effect replacing and releasing the originally condensed counterions in solution (i.e. those bound to the DNA and to cationic membranes) [20].

Aside from DOPC, a commonly used neutral lipid in CL-DNA mixtures is DOPE (dioleoyl-phosphadtidylethanolamine) (figure 2). The main difference in the chemical structure of these two lipids is the much smaller headgroup size for DOPE. This difference leads to an inverse cone shaped DOPE lipid (favoring the inverse hexagonal H_{II} phase) in contrast to the cylindrical shaped DOPC and DOTAP lipids (favoring the lamellar structure). SAXS data from DOTAP/DOPC/DOPE-DNA complexes showed the onset of a structural transition from the L_α^C phase to a new liquid-crystalline phase as a function of increasing Φ_{DOPE} (weight fraction of DOPE) at constant DOTAP/DNA [37].

At Φ_{PE} = 0.26 SAXS showed the presence of the lamellar L_α^C structure similar to what was described above. For 0.7 <Φ_{PE} < 0.85 the peaks of the SAXS scans of the CL-DNA complexes were indexed on a 2D hexagonal lattice with unit cell spacing a ≈ 67.4 Å [37]. The structure was found to be consistent with a 2D columnar inverted hexagonal phase of CL-DNA complexes, termed H_{II}^C (Figure 4). In the H_{II}^C phase DNA chains are inserted

within the lumen of inverse cylindrical micelles, which, in turn, are arranged on a hexagonal lattice. The structure is similar to the inverted hexagonal H_{II} phase of DOPE in excess water [38, 39]. Assuming a lipid monolayer thickness of 20 Å, the diameter of the lumen of the inverse micelles is ≈ 28 Å, which is sufficient for a DNA molecule with approximately two hydration shells.

2.1 Transfection efficiency of lamellar L_α^C and inverse hexagonal H_{II}^C phases

A major goal of research on CL-DNA complexes is to elucidate the correlation between the different liquid crystalline structures and transfection efficiency (TE). In a series of comprehensive studies TE was indeed found to be structure dependent. In particular, it was found that for lamellar CL-DNA complexes the membrane charge density σ_M is a universal parameter predictive of TE [40, 31]. In contrast, while TE of non-lamellar H_{II}^C phases is relatively large, it is independent of σ_M, which implies a distinctly different transfection mechanism involving different interactions between complexes and cellular components [40].

To study the dependence of TE on σ_M a series of multivalent lipids (MVLs) were custom synthesized (figure 5), which allowed for systematic variation of the charge (between 2+ and 5+) and size of the lipid headgroup [41–43]. CL-DNA complexes with membranes consisting of mixtures of DOPC and the MVLs shown in figure 5 were found to form the lamellar phase [40].

Figure 6 shows the transfection efficiency of the MVL/DOPC-DNA complexes plotted versus the membrane charge density, σ_M ($\sigma_M = [1-\Phi_{nl}/(\Phi_{nl} + r\Phi_{cl})]\sigma_{cl}$), at the cationic lipid/DNA charge ratio $\rho_{chg} = 2.8$ [40]. Here, $r = A_{cl}/A_{nl}$ is the ratio of the headgroup areas of the cationic and the neutral lipid; $\sigma_{cl} = eZ/A_{cl}$ is the charge density of the cationic lipid with valence Z; Φ_{nl} and Φ_{cl} are the mole fractions of the neutral and cationic lipids, respectively. For this study the membrane charge density was varied by changing the amount of neutral lipid while keeping the amount of DNA and cationic lipid per sample constant. The membrane charge density was calculated using $A_{nl} = 72$ Å^2, $r_{DOTAP} = 1$, $r_{MVL2} = 1.05 \pm 0.05$, $r_{MVL3} = 1.30 \pm 0.05$, $r_{MVL5} = 2.3 \pm 0.1$, $r_{TMVL5} = 2.5 \pm 0.1$, $Z_{DOTAP} = 1$, $Z_{MVL2} = 2.0 \pm 0.1$, $Z_{MVL3} = 2.5 \pm 0.1$, $Z_{MVL5} = Z_{TMVL5} = 4.5 \pm 0.1$ [40]. The solid curve in figure 6, which fits the TE data well describes a Gaussian $TE = TE_0 + A \exp-[(\sigma_M - \sigma_M^*)/w]^2$, with optimal charge density $\sigma_M^* = 17.0\pm0.1 \times 10^{-3}$ e/Å^2, $TE_0 = -(2.4\pm0.4) \times 10^7$ RLU/mg protein $A = 9.4\pm0.6 \times 10^8$ RLU/mg protein, and $w = 5.8\pm0.5 \times 10^{-3}$ e/Å^2 [40]. As is evident TE of all MVL containing complexes, when plotted versusσ_M, merge onto a single curve. This identifies σ_M as a universal parameter for transfection by lamellar L_α^C CL-DNA complexes (i.e. a predictor of TE) [40].

The simplest model describing the L_α^C phase TE behavior postulates that an increase in σ_M (figure 6, regime I) enhances fusion between the cationic membranes of lamellar complexes (trapped in endosomes) and anionic endosomal membranes facilitating release of complexes to the cell cytoplasm. However, a very largeσ_M (figure 6, regime III) inhibits cationic membranes from efficiently releasing anionic DNA upon cell entry after endosomal escape. This then gives rise to the optimal σ_M (regime II) observed in experiments (i.e. σ_M just large enough to fuse with and escape the endosome but not too large to prevent complex dissociation upon cell entry) [40]. In contrast, it was found that TE of DOTAP/DOPE H_{II}^C complexes (figure 6 open circle) is independent of σ_M, with the high TE likely related to the efficient fusion between the membranes of complexes containing DOPE and cellular membranes (e.g. the endosomal membranes allowing delivery of complexes to the cytoplasm) [31].

3. Hexagonally ordered cylindrical micelles embedded in a DNA honeycomb lattice: dendritic lipid cationic liposome-DNA complexes for gene delivery

As studies of the $L_\alpha C$ and H_{II}^C phases showed, the shape of the membrane component of the complex often determines the structure of CL-DNA complexes. Membrane shape, in turn, is often (but not always) determined by the spontaneous curvature of the membrane [38, 39], which is related to the molecular shape of the constituent lipids [36]. To develop the H_I^C phase of CL-DNA complexes (i.e. containing cylindrical micelles with positive curvature) a highly charged (16+) multivalent cationic lipid with a dendritic headgroup, labeled MVLBG2, was synthesized (figure 7, top left) [42,44].

Complexes of DNA with mixtures of MVLBG2 and DOPC were found to exhibit the lamellar L_α^C phase at 10 mol% MVLBG2. Most interestingly, in a narrow range of composition ≈ 25 mol% MVLBG2, a new type of liquid crystalline structure was observed where the SAXS peaks indexed precisely onto a 2D hexagonal lattice (figure 7, bottom) [44]. In this structure, termed H_I^C, hexagonally arranged rod-shaped lipid micelles are surrounded by DNA forming a continuous substructure with honeycomb symmetry (figure 7, top right) [44]. The large headgroup of MVLBG2 forces the lipid to assemble into cylindrical lipid micelles that are arranged on a hexagonal lattice, with an interaxial distance of 81.5 Å. The diameter of the rod-shaped micelles estimated to be around 41 Å is consistent with the thickness of a bilayer formed by these lipids [44]. The hydrated DNA rods, with a diameter ≈ 25 Å, are arranged on a honeycomb lattice in the interstices of the lipid micelle arrangement. The remaining interstitial space is filled by the headgroups, water and counterions. Interestingly, the DNA forms a three-dimensionally contiguous substructure in the H_I^C phase, as opposed to isolated DNA rods and DNA sheets in the H_{II}^C and L_α^C phases, respectively (figures 4 and 3).

At larger mole fractions of MVLBG2, $0.5 > \Phi_{MVLBG2}$ (mol fraction) > 0.3, SAXS data shows the onset of a distorted hexagonal H_I^C phase [45]. Most interestingly, both the H_I^C and the distorted H_I^C phases both show enhanced transfection efficiency, which deviates from the universal Bell curve observed for lamellar complexes (figure 6) [44,45]. This suggests a distinctly new mechanism of action for these dendritic lipid–DNA complexes, which remains to be understood.

4. Highly efficient gene silencing activity of short-interfering RNA (siRNA) embedded in a double gyroid cubic lipid phase

Recently, a major new branch in cationic lipid-based nucleic acid research worldwide has arisen following the discovery of RNA interference (RNAi) as a post-transcriptional gene-silencing pathway [46–52]. Short strands of double-stranded RNA (19–25 bp, with two 3-primed-nucleotide overhangs, termed short-interfering RNA, siRNA), when complexed with cationic liposomes, evoke the RNA interference pathway leading to gene silencing [48, 51–53]. In addition to its wide spread applications in functional genomics, siRNA technology promises to revolutionize biotechnology and therapeutics [50–52]. However, the current limiting step in realizing the full potential of siRNA gene silencing technology is the development of efficient chemical carriers of siRNA [52, 53]. Furthermore, current lipid-carriers typically impart an unacceptable level of cell toxicity, which is due to the high membrane charge required for efficient cytoplasmic cell delivery [53].

In recent work a method was developed to produce a novel bicontinuous double gyroid cubic lipid phase, which incorporates functional gene silencing siRNA within its two water

channels (figure 8, left) [54, 55]. The inverse bicontinuous cubic structure was established by synchrotron x-ray scattering (figure 8, middle).

Cubic phase forming lipids favor saddle-splay shaped surfaces with negative curvature (i.e. $C_1C_2 < 0$). Such negative Gaussian curvatures are also characteristic of membrane pores [56]. Thus, it was hypothesized that when brought into contact with a membrane barrier (such as endosomal membranes after endocytosis of complexes), cubic phase complexes should give rise to enhanced membrane fusion, because such a process leads naturally to the formation of pores with the desired negative Gaussian curvature interface [31, 54–56].

The cubic gyroid phase was indeed found to be highly efficient in cytoplasmic delivery of CL-siRNA complexes leading to sequence-specific gene silencing at low cell toxicity (figure 8, right). This significant discovery is consistent with the aforementioned hypothesis that the cubic phase lipids' tendency for pore formation leads to fusion of the membranes of the gyroid lipid-siRNA complex and endosomal membranes upon endocytosis. Pores, in turn, allow for efficient cytoplasmic siRNA delivery leading to gene silencing. Interestingly, because the mechanism of fusion is independent of membrane charge density, gyroid cubic complexes enable efficient endosomal escape of complexes even at very low membrane charge (unlike the lamellar $L_\alpha{}^C$ complexes which show enhanced TE only at relatively high membrane charge densities).

In other recent work on CL-short nucleic acid complexes the formation of an entirely new type of 2D liquid crystalline phase was described, when double-stranded siRNA was replaced with similar short DNA confined between membranes of the $L_\alpha C$ phase [57]. Remarkably, it was found that unexpectedly large end-to-end interactions set in between 11 bp DNA rods when overhangs are reduced from 10T or 5T to 2T, which, in turn, leads to the formation of a novel 2D columnar nematic phase with finite-length columns consisting of stacks of on average four short DNA molecules. This finding is expected to have broad implications in the future design of optimally packed delivery vectors for small anisotropic molecules (e.g. active peptides and small proteins) for applications in bio-nanotechnology and chemical delivery.

5. Concluding remarks

The long-term objective of the studies described in this review of liquid crystalline cationic liposome-nucleic acid complexes, is to develop a fundamental science base, which will lead to the design and synthesis of optimal lipid carriers of DNA and short-interfering RNA for gene delivery, gene silencing, and disease control. The structure-function data obtained from such studies should eventually allow one to begin the formidable task of a rational design of these self assemblies for enhanced nucleic acid delivery applications from the ground up beginning with the chemical structure of the lipids and the correct compositions in mixtures including functional DNA and RNA. We expect that future experiments will focus on improving transfection efficiencies of synthetic carriers by developing insights into transfection-related mechanisms at the individual complex level, in particular, clarifying the spatial and temporal distribution of CL-nucleic acid complexes in the cytoplasm, their mechanisms of transport, and mechanisms of release of nucleic acids possibly due to interactions with cell macromolecular components.

Aside from the medical and biotechnological ramifications in gene therapy and gene and drug therapeutics, the research should also shed light on other problems in biology. The development of efficient human-artificial-chromosome vectors in the future, which will most likely occur once efficient synthetic delivery systems have been further optimized, is a long range goal in studies designed to characterize chromosome structure and function. Furthermore, molecular biology studies would benefit substantially from the ability of

transfecting hard to transfect cell lines with synthetic delivery systems; for example, in studies designed to characterize the structure of promoters of human genes in the appropriate cell lines.

Acknowledgments

Support is acknowledged by the U.S. National Institutes of Health GM-59288 (structure–biological activity studies), the U.S. National Science Foundation DMR-1101900 (lipid phase behavior), and the U.S. Department of Energy-Basic Energy Sciences grant number DOE-DE-FG02-06ER46314 (liposome–nucleic acid phase structure). CL was funded by the Swedish Research Council (VR) and in part by the US DOE-BES. The X-ray diffraction work was carried out at the Stanford Synchrotron Radiation Laboratory (SSRL) beam lines 7.2 and 4.2. CRS acknowledges useful discussions with KAIST Faculty where he has a WCU (World Class University) Visiting Professor of Physics appointment supported by the National Research Foundation of Korea funded by the Ministry of Education, Science and Technology No. R33-2008-000-10163-0.

References

1. Bielke, W.; Erbacher, C., editors. Nucleic Acid Transfection. Vol. 296. Springer; Heidelberg: 2010. Topics in Current Chemistry.
2. Ewert KK, Zidovska A, Ahmad A, Bouxsein NF, Evans HM, McAllister CS, Samuel CE, Safinya CR. Topics Curr Chem. 2010; 296:191–226.
3. Safinya CR, Ewert KK, Ahmad A, Evans HM, Raviv U, Needleman DJ, Lin AJ, Slack NL, George CX, Samuel CE. Phil Transact Royal Soc A. 2006; 364:2573–2596.
4. Huang, L.; Hung, M-C.; Wagner, E., editors. Non-Viral Vectors for Gene Therapy. Vol. 53. Vol. 2. Elsevier; San Diego: 2005. Advances in Genetics.
5. Ewert K, Ahmad A, Evans HM, Safinya CR. Expert Opin Biol Ther. 2005; 5:33–53. [PubMed: 15709908]
6. Ewert, K.; Evans, HM.; Ahmad, A.; Slack, NL.; Lin, AJ.; Martin-Herranz, A.; Safinya, CR. Non-viral Vectors for Gene Therapy. In: Huang, L.; Hung, M-C.; Wagner, E., editors. Advances in Genetics. 2. Vol. 53. Elsevier; London: 2005. p. 117-153.
7. Ewert K, Slack NL, Ahmad A, Evans HM, Lin AJ, Samuel CE, Safinya CR. Curr Med Chem. 2004; 11:133–149. [PubMed: 14754413]
8. Mahato, RI.; Kim, SW., editors. Pharmaceutical Perspectives of Nucleic Acid-Based Therapeutics. Taylor and Francis; New York: 2002.
9. Chesnoy S, Huang L. Annu Rev Biophys Biomol Struct. 2000; 29:27–47. [PubMed: 10940242]
10. Huang, L.; Hung, M-C.; Wagner, E., editors. Nonviral Vectors for Gene Therapy. Academic Press; San Diego: 1999.
11. Felgner PL, Gader TR, Holm M, Roman R, Chan HW, Wenz M, Northrop JP, Ringold GM, Danielsen M. Proc Natl Acad Sci USA. 1987; 84:7413–7417. [PubMed: 2823261]
12. Nabel GJ, Nabel EG, Yang ZY, Fox BA, Plautz GE, Gao X, Huang L, Shu S, Gordon D, Chang AE. Proc Natl Acad Sci USA. 1993; 90:11307–11311. [PubMed: 8248244]
13. Edelstein ML, Abedi MR, Wixon J. J Gene Med. 2007; 9:833–842. [PubMed: 17721874]
14. Gene Therapy Clinical Trials Worldwide. [accessed Sep 6, 2011] The journal of gene medicine clinical trial site. 2011. http://www.wiley.com/legacy/wileychi/genmed/clinical/
15. Williams DA, Baum C. Science. 2003; 302:400–401. [PubMed: 14563994]
16. Thomas CE, Ehrhardt A, Kay MA. Nature Rev Genet. 2003; 4:346–358. [PubMed: 12728277]
17. Hacein-Bey-Abina S, Garrigue A, Wang GP, Soulier J, Lim A, Morillon E, Clappier E, Caccavelli L, Delabesse E, Beldjord K, Asnafi V, MacIntyre E, Cortivo LD, Radford I, Brousse N, Sigaux F, Moshous D, Hauer J, Borkhardt A, Belohradksy DH, Wintergerst U, Velez MC, Leiva L, Sorensen R, Wulffraat N, Blanche S, Bushman FD, Fischer A, Cavazzana-Calvo M. J Clin Invest. 2008; 118:3132–3142. [PubMed: 18688285]
18. Harrington JJ, Van Bokkelen G, Mays RW, Gustashaw K, Willard HF. Nature Genetics. 1997; 15:345–355. [PubMed: 9090378]
19. Roush W. Science. 1997; 276:38–39. [PubMed: 9122708]

20. Rädler JO, Koltover I, Salditt T, Safinya CR. Science. 1997; 275:810–814. [PubMed: 9012343]
21. Safinya CR, Roux D, Smith GS, Sinha SK, Dimon P, Clark NA, Bellocq AM. Phys Rev Lett. 1986; 57:2718–2721. [PubMed: 10033843]
22. Roux D, Safinya CR. J Phys (Paris). 1988; 49:307–318.
23. Safinya CR, Sirota EB, Roux D, Smith GS. Phys Rev Lett. 1989; 62:1134–1137. [PubMed: 10039585]
24. Lei N, Safinya CR, Bruinsma RF. J Phys II. 1995; 5:1155–1163.
25. Salditt T, Koltover I, Rädler JO, Safinya CR. Phys Rev Lett. 1997; 79:2582–2585.
26. Salditt T, Koltover I, Rädler JO, Safinya CR. Phys Rev E. 1998; 58:889–904.
27. Koltover I, Salditt T, Safinya CR. Biophys J. 1999; 77:915–924. [PubMed: 10423436]
28. Safinya CR. Curr Opin Struct Biol. 2001; 11:440–448. [PubMed: 11495736]
29. De Gennes, PG.; Prost, J. The Physics of Liquid Crystals. 2. Oxford University Press; Oxford: 1993.
30. Chaikin, PM.; Lubensky, TC. Principles of Condensed Matter Physics. Cambridge University Press; Cambridge: 1995.
31. Lin AJ, Slack NL, Ahmad A, George CX, Samuel CE, Safinya CR. Biophys J. 2003; 84:3307–3316. [PubMed: 12719260]
32. O'Hern C, Lubensky T. Phys Rev Lett. 1998; 80:4345–4348.
33. Golubović L, Golubović M. Phys Rev Lett. 1998; 80:4341–4344.
34. Golubović L, Lubensky T, O'Hern C. Phys Rev E. 2000; 62:1069–1094.
35. Manning GS. J Chem Phys. 1969; 51:924–933.
36. Israelachvili, JN. Intermolecular and Surface Forces. 2. Academic Press; London: 1992.
37. Koltover I, Salditt T, Rädler JO, Safinya CR. Science. 1998; 281:78–81. [PubMed: 9651248]
38. Seddon JM. Biochim Biophys Acta. 1989; 1031:1–69. [PubMed: 2407291]
39. Gruner SM. J Phys Chem. 1989; 93:7562–7570.
40. Ahmad A, Evans HM, Ewert K, George CX, Samuel CE, Safinya CR. J Gene Med. 2005; 7:739–748. [PubMed: 15685706]
41. Ewert K, Ahmad A, Evans HM, Schmidt HW, Safinya CR. J Med Chem. 2002; 45:5023–5029. [PubMed: 12408712]
42. Ewert KK, Evans HM, Zidovska A, Bouxsein NF, Ahmad A, Safinya CR. Bioconjugate Chem. 2006; 17:877–888.
43. Schulze U, Schmidt HW, Safinya CR. Bioconjugate Chem. 1999; 10:548–552.
44. Ewert KK, Evans HM, Zidovska A, Bouxsein NF, Ahmad A, Safinya CR. J Am Chem Soc. 2006; 128:3998–4006. [PubMed: 16551108]
45. Zidovska A, Evans HM, Ewert KK, Quispe J, Carragher B, Potter CS, Safinya CR. J Phys Chem B. 2009; 113:3694–3703. [PubMed: 19673065]
46. Fire A, Xu SQ, Montgomery MK, Kostas SA, Driver SE, Mello CC. Nature. 1998; 391:806–811. [PubMed: 9486653]
47. Cogoni C, Macino G. Curr Opin Genet Dev. 2000; 10:638–643. [PubMed: 11088014]
48. Elbashir SM, Harborth J, Lendeckel W, Yalcin A, Weber K, Tuschl T. Nature. 2001; 411:494–498. [PubMed: 11373684]
49. Caplen NJ, Parrish S, Imani F, Fire A, Morgan RA. Proc Natl Acad Sci USA. 2001; 98:9742–9747. [PubMed: 11481446]
50. See e.g., Hannon GJ, Rossi JJ. Nature. 2004; 431:371–378. [PubMed: 15372045]
51. Karagiannis TC, El-Osta A. Cancer Gene Ther. 2005; 12:787–795. [PubMed: 15891770]
52. Sioud M. Trends Pharm Sci. 2004; 25:22–28. [PubMed: 14723975]
53. Bouxsein NF, McAllister CS, Ewert KK, Samuel CE, Safinya CR. Biochemistry. 2007; 46:4785–4792. [PubMed: 17391006]
54. Leal C, Bouxsein NF, Ewert KK, Safinya CR. J Am Chem Soc. 2010; 132:16841–16847. [PubMed: 21028803]

55. Leal C, Ewert KK, Shirazi RS, Bouxsein NF, Safinya CR. Langmuir. 2011; 27:7691–7697. [PubMed: 21612245]

56. Siegel DP. Biophys J. 1999; 76:291–313. [PubMed: 9876142]

57. Bouxsein NF, Leal C, McAllister CS, Ewert KK, Li Y, Samuel CE, Safinya CR. J Am Chem Soc. 2011; 133:7585–7595. [PubMed: 21520947]

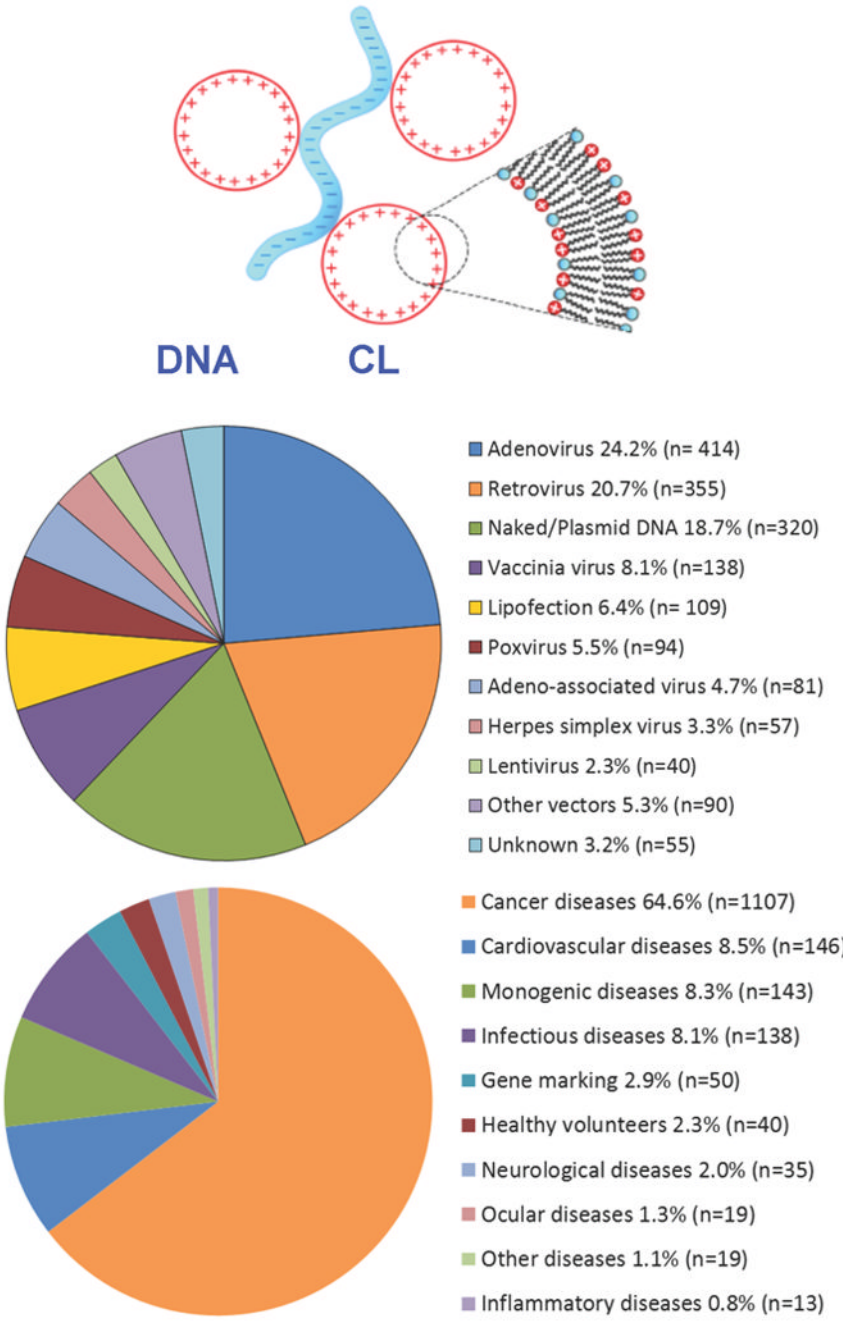

Figure 1.

(**Top**) Schematic of cationic liposomes (or vesicles, containing a bilayer of lipid molecules, usually a mixture of cationic and neutral lipids) attached to anionic DNA with an overall positive charge. (**Middle**) Ongoing gene therapy clinical trials worldwide separated by carrier (or vector) type (n denotes number of trials). Cationic lipid based vectors termed “lipofection” constitute about 6.4% of clinical trials. (**Bottom**) Gene therapy trials separated by targeted disease. Lipofection is often used to target cancer and monogenic diseases. Pie graphs adapted from http://www.wiley.com/legacy/wileychi/genmed/clinical/ [14].

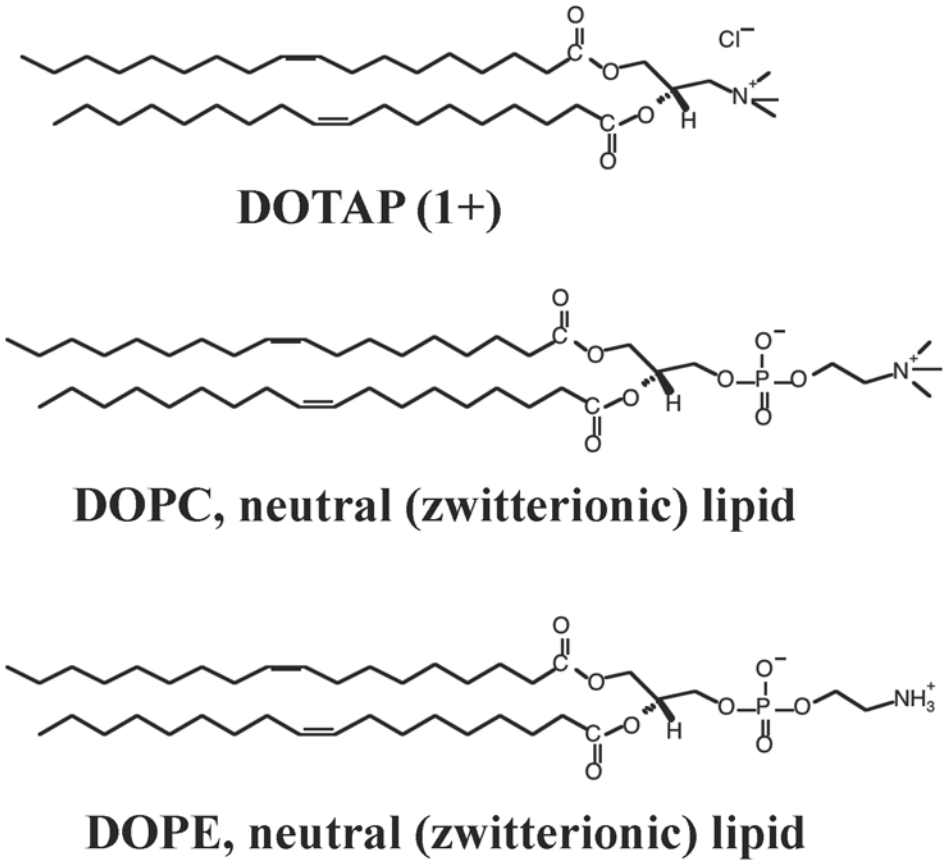

Figure 2.
(**Top**) Cationic lipid DOTAP (dioleoyl trimethylammonium propane). (**Middle**) Neutral lipid DOPC (dioleoyl-phosphatidylcholine). (**Bottom**) Neutral lipid DOPE (dioleoyl-phosphadtidylethanolamine).

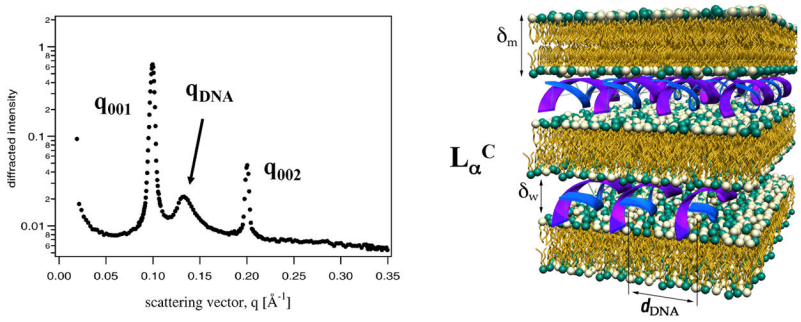

Figure 3.

(**Left**) A high-resolution synchrotron SAXS scan of cationic liposome-DNA (CL-DNA) complexes in excess water at total lipid (DOTAP + DOPC) to DNA weight ratio (L/D) of 7. The membrane composition was DOTAP/DOPC 1:1 (wt.:wt.). The complexes were prepared at the isoelectric point of the complex with DOTAP/DNA = 2.2 (wt.:wt.). The Bragg reflections at q_{001} = 0.098 $Å^{-1}$ and q_{002}= 0.196 $Å^{-1}$ result from the multilamellar $L_\alpha{}^c$ structure with intercalated monolayer DNA (see schematic at right). The intermediate broad DNA-DNA correlation peak at q_{DNA} results from the average interaxial spacing d_{DNA} (see schematic at right). (**Right**) Schematic of the lamellar $L_\alpha{}^C$ phase with alternating lipid bilayer-DNA monolayer of cationic lipid-DNA (CL-DNA) complexes as described in the text. The interlayer spacing is $d = \delta_w + \delta_m$. Reprinted with permission from [20]. Copyright 1997 Science.

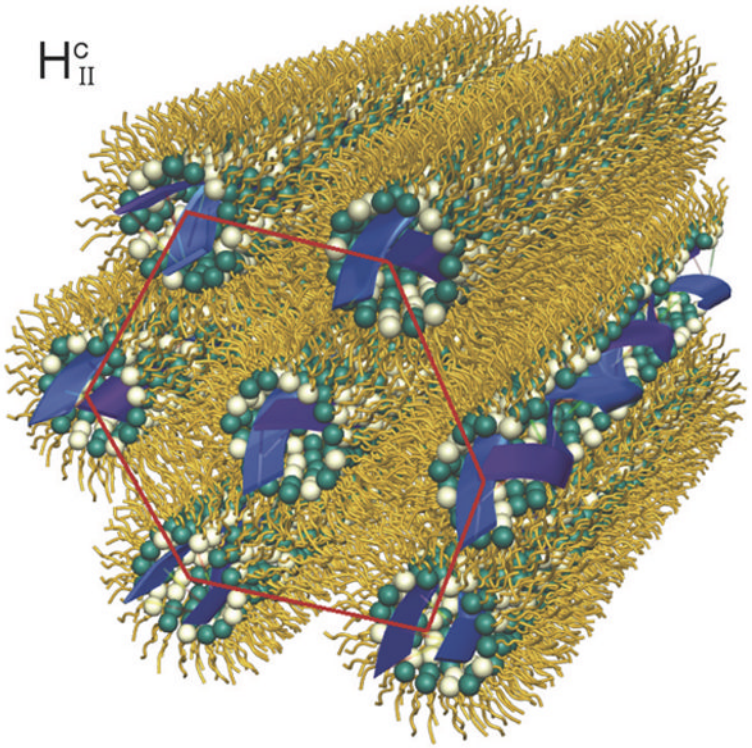

Figure 4.
Schematic of the inverted hexagonal H_{II}^{C} phase of cationic lipid-DNA (CL-DNA) complexes. In this phase, cylinders consisting of DNA coated with an inverse lipid monolayer are arranged on a hexagonal lattice. Reprinted with permission from [37]. Copyright 1998 Science.

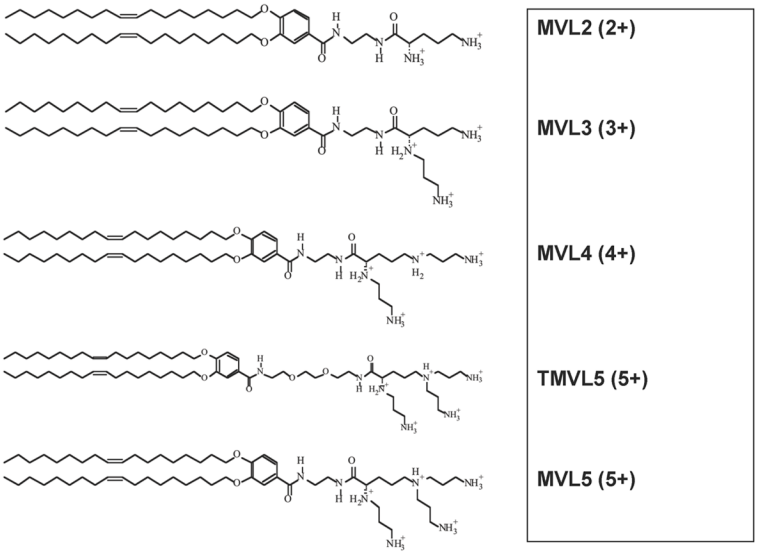

Figure 5.
Chemical structure and maximum charge of custom synthesized multivalent lipids (MVLs). Adapted from [41].

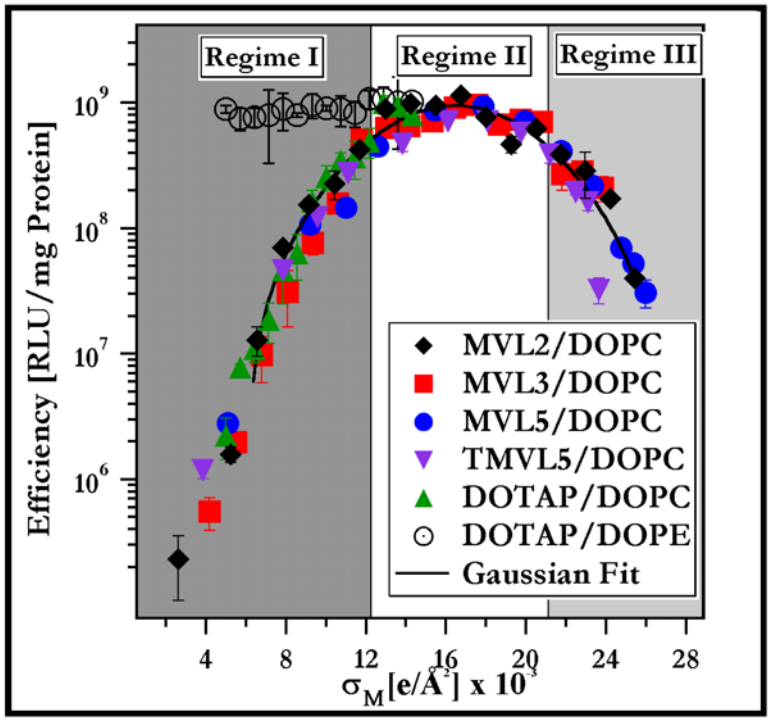

Figure 6.

Transfection efficiency (TE) as a function of the membrane charge density, σ_M (= average charge per unit area of the membrane; see text for definition) for lamellar CL-DNA complexes prepared with MVL2, MVL3, MVL5, TMVL5, and DOTAP (see figures 2 and 5). All data are for mouse fibroblast cell lines. All data were taken at cationic lipid/DNA charge ratio ρ_{chg} = 2.8. Thus, the TE of the lamellar L_α^C complexes may be described by a universal, bell-shaped curve as a function of σ_M (the solid line is a Gaussian fit to the data). TE data for DOTAP/DOPE complexes (open circles, H_{II}^C phase) deviate from the universal curve, indicative of a distinctly different transfection mechanism for the inverted hexagonal phase. Three regimes of transfection efficiency are labeled as described in the text. Reprinted with permission from [40]. Copyright 2005 John Wiley & Sons, Ltd.

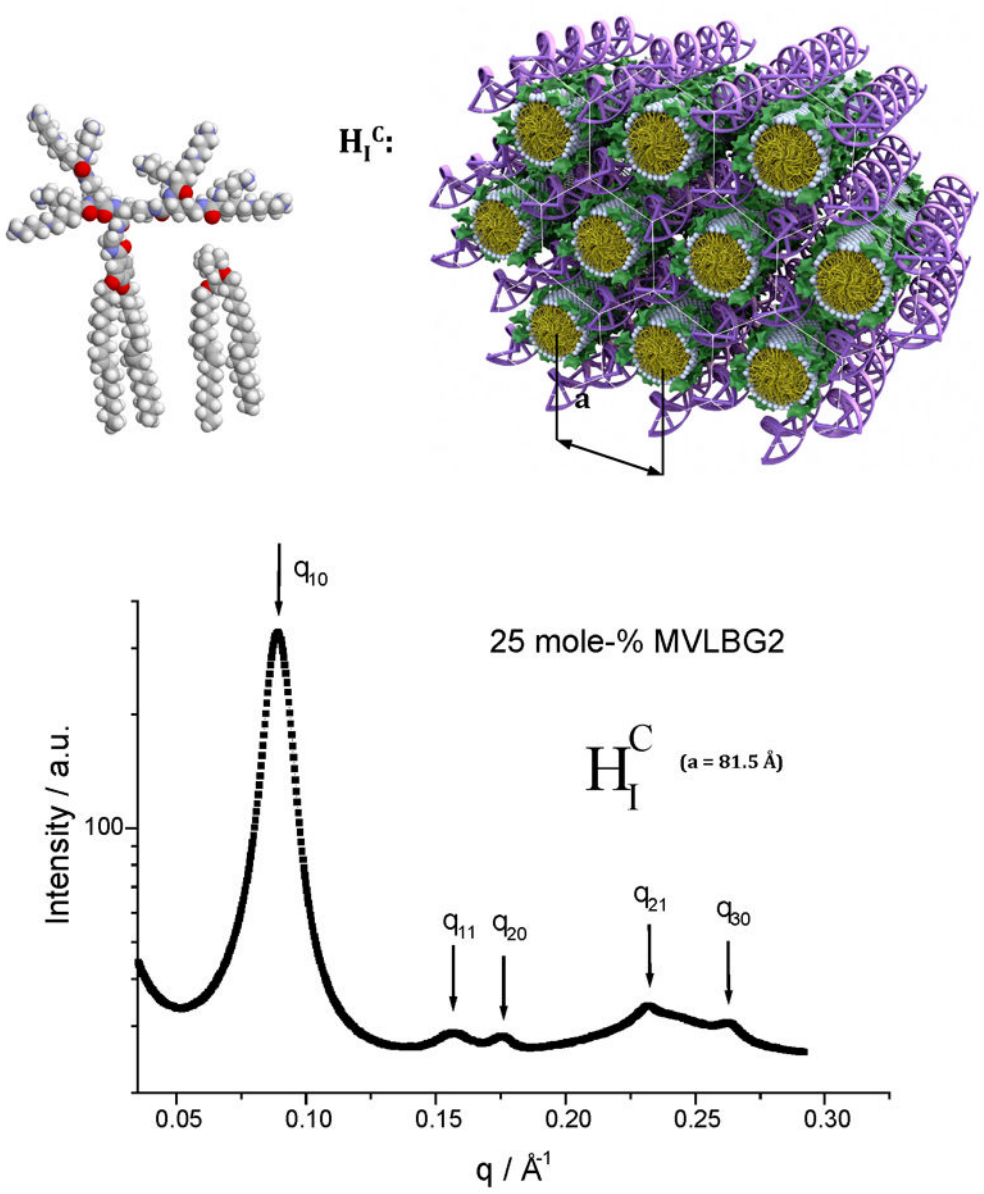

Figure 7.

(**Top left)** Molecular models of hexadecavalent MVLBG2 and monovalent DOTAP. **(Top right)** Schematic of the H_I^C phase of CL-DNA complexes. In this phase, oppositely charged DNA chains surround cylindrical micelles arranged on a hexagonal lattice. **(Bottom)** Synchrotron x-ray scattering pattern of MVLBG2/DOPC-DNA complexes with 25 mol % of the highly charged dendritic lipid MVLBG2. The SAXS peaks index to a 2D hexagonal lattice. The highly cone-shaped MVLBG2 results in the formation of the H_I^C phase with cylindrical micelles with a positive curvature along one direction. Reprinted with permission from [44]. Copyright 2006 American Chemical Society.

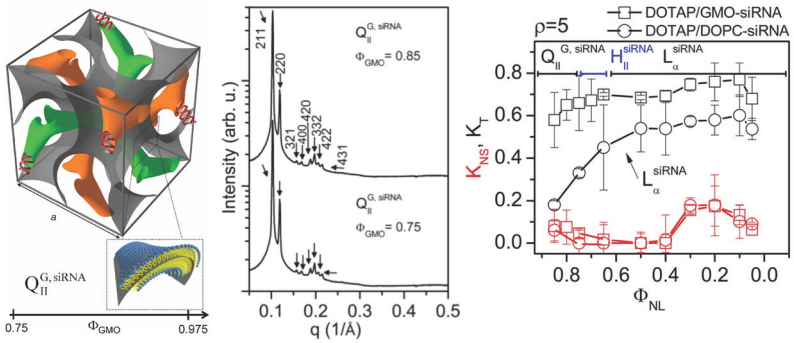

Figure 8.

(**Left**) The double gyroid lipid cubic phase incorporating functional short-interfering RNA (siRNA) within its two (green and orange) water channels. This new phase, labeled $Q_{II}^{G,siRNA}$, is obtained for DOTAP/GMO-siRNA complexes for GMO molar fractions (Φ_{GMO}) of $0.75 \leq \Phi_{GMO} \leq 0.975$. (The non-ionic lipid glycerol monooleate (GMO, 1-monooleoyl-glycerol) is a cubic phase forming lipid.) A lipid bilayer surface separates the two intertwined but independent water channels. For clarity, the bilayer (which has a negative Gaussian curvature $C_1C_2 < 0$) is represented by a surface (grey) corresponding to a thin layer in the center of the membrane as indicated in the enlarged inset. (**Middle**) Synchrotron small-angle X-ray scattering (SAXS) data obtained for DOTAP/GMO in 30 wt % water containing functional short RNA molecules at $\Phi_{GMO} = 0.75$ (below) and at $\Phi_{GMO} = 0.85$ (above). The large number of reflections result from a body centered gyroid cubic structure labeled $Q_{II}^{G,\,siRNA}$ (space group Ia3d). (**Right**) Total specific and nonspecific gene knockdown (K_T, black lines and symbols) and nonspecific gene knockdown (K_{NS}, red lines and symbols) for DOTAP/GMO-siRNA complexes (squares) and DOTAP/DOPC-siRNA complexes (circles) as a function of mole fraction of neutral lipid (Φ_{NL}). Optimal silencing corresponds to K_T approaching 1 and K_{NS} approaching 0. DOTAP/GMO-siRNA complexes in the gyroid cubic phase at low cationic lipid content ($Q_{II}^{G,\,siRNA}$, $\Phi_{GMO} \geq 0.75$) show remarkably improved sequence-specific gene silencing over complexes in the lamellar phase (L_α^{siRNA}). Reprinted with permission from [54]. Copyright 2010 American Chemical Society.